THE PUBLISHING HOUSE
OF THE ROMANIAN ACADEMY

PROCEEDINGS OF THE ROMANIAN ACADEMY, Series A,
Volume 24, Number 1/2023, pp. 93–102
DOI: 10.59277/PRA-SER.A.24.1.11

WELD LINE STRUCTURED LIGHT STRIPE CENTER EXTRACTION APPROACH BASED ON DATA DIMENSIONALITY REDUCTION

Qingchun ZHENG[1,2], Qipei LIU[1,2], Peihao ZHU[1,2,*], Hao SHI[1,2], Xiaoyang LI[1,2]

[1] Tianjin University of Technology, Tianjin Key Laboratory for Advanced Mechatronic System Design and Intelligent Control, School of Mechanical Engineering, Tianjin 300384, China
[2] Tianjin University of Technology, National Demonstration Center for Experimental Mechanical and Electrical Engineering Education
Corresponding author: Peihao ZHU, E-mail: zhupeihao_gp@163.com

Abstract. In order to improve the accuracy and speed of extracting the center of the line structured light stripe when using the vision measurement technology to get the 3D information of the weld sample, this paper proposes a center extraction approach based on the idea of data dimensionality reduction. First, use the weighted gray centroid approach to get the initial center point of the light stripe. Then, build a 7×7 template centered on the pixel block where the initial point is located and performs singular value decomposition on the 49×3 matrix within the template to get the normal direction of the initial point. Finally, calculate the stripe's exact center points through second-order Taylor expansion and smooth repair by cubic spline interpolation of breakpoints. The comparison experimental results show that this approach can effectively reduce the influence of the noise outside the light stripe on the center extraction, reduce the extraction time while ensuring the measurement accuracy, which can lay a good foundation for the point cloud data processing and surface reconstruction.

Key words: line structured light, Steger approach, gray centroid approach, data dimensionality reduction, singular value decomposition.

1. INTRODUCTION

Welding technology has an indispensable role in industrial production, and the quality of the weld directly affects the life of the parts and structural safety. We can judge the quality of the weld by identifying surface defects that arise during the welding process. For welds that cannot meet surface quality requirements, grinding is essential. Currently, the detection and polishing of the weld mostly rely on manual, which is prone to judgment errors caused by subjectivity and cannot achieve real-time, accurate grinding of complex welds. Besides, the work environment is harsh and has high labor intensity, which cannot guarantee workers' work continually. With the continuous development of intelligent manufacturing technology, automated systems gradually replace manual grinding, mainly by robots. Currently, most industrial robots perform their work mainly with the help of a demonstrator [1]. To promote the robot's perception and environmental adaptability, it is necessary to provide the required parameters for the force-controlled grinding of complex surface welds to the robot with the help of vision measurement technology.

As a branch of active vision measurement technology, line structured light is widely used in non-contact precision measurement because of its wide measurement range, ease of use, good monochromaticity, and high luminance showing high robustness to objects with complex surface textures [2]. The line structured light vision measurement platform often comprises a one-dimensional or multi-dimensional moving platform, an industrial camera and a laser transmitter [3]. Because of its attributes of non-contact, high-speed, and high-accuracy, etc. [4], it is suitable for achieving complete measurement of complex surfaces. Besides, because the extraction error of the light stripe center determines the 3D reconstruction accuracy, that fast and accurate stripe center extraction from the image is the most critical step to achieving the measurement of the weld sample [5].

We can divide the center extraction approaches of line structured light into pixel-level and sub-pixel-level accuracy. Among them, the pixel-level extraction approaches mainly include the extreme value approach [6], the direction template approach [7], and the curve fitting approach [8]. Such approaches are simple and easy to achieve but are disturbed by noise easily. Therefore, this kind of approach can't meet the demands of high-precision measurement.

The standard sub-pixel extraction approaches mainly include the gray centroid approach and the Steger approach. Wang *et al*. [9] used the difference image and region growth approach to reduce the influence of uneven background and speckle noise, then used the gray centroid approach to extract the initial center of the light stripe, which has strong robustness. Guo [10] used the brightness enhancement approach and the improved Otsu threshold segmentation approach to improve image quality. Then, use the gray centroid approach and slice fitting approach to get a robust and smooth centerline. Although the gray centroid approach can quickly get the sub-pixel coordinates of the center point, because it can't effectively overcome the influence of noise, it still lacks extraction accuracy. Steger [11] proposed a centerline extraction approach based on the Hessian matrix. The core of this approach is to get the normal direction of the light stripe by calculating the Hessian matrix, and get the center point coordinates under sub-pixel accuracy by calculating the extreme value in the normal direction, and has high accuracy and robustness [12]. However, because it needs to carry out five times of two-dimensional Gaussian convolution on the image to calculate the normal, the amount of operation is enormous. To solve this problem, Hu *et al*. [13] proposed a approach based on adaptive threshold power transformation, which improved the extraction speed and met the requirements of real-time extraction in the industry. Liu *et al*. [14] proposed a approach for extracting the center of the light stripe based on the Hessian matrix and region growth approach. Although this approach can extract the stripe center accurately, it is not sensitive to the object surface with strong optical properties.

In summary, how to guarantee the extraction accuracy while satisfying the extraction speed in the process of center extraction is the key of many scholars' research. To address this critical problem, this paper proposes a center extraction approach. The main contribution of this paper as follows: Use the singular value decomposition to get the normal directions of the target pixel points, which enhances the operation speed while ensuring the accuracy of the extraction approach.

The rest of this paper is organized as follows: Section 2 analyzes the characteristics of line structured light and the principle and process of this approach; Section 3 conducts the experiment of center extraction and examines the accuracy of the results, and Section 4 is the conclusion of this paper.

2. APPROACH DESCRIPTION

2.1. Basic theory

Currently, common point or line structured light emitters mainly comprise He-Ne lasers and lenses. The directionality of the output light of He-Ne lasers is well, and the combination of a columnar mirror can make the emitted beam diverge in one direction, forming a structured light tangent plane whose thickness is uniform at a closer distance. Since the output spot of the He-Ne laser is Gaussian distributed, the light intensity of the diverging light plane at the interface perpendicular to it can also be Gaussian distributed. The light intensity distribution is:

$$G(x)=\frac{1}{\sqrt{2}\pi\sigma}\exp\left[-\frac{(x-\mu)^2}{2\delta^2}\right] \tag{1}$$

The middle of the beam is the brightest, and the brightness gradually decreases from the center to the edge. According to the knowledge of computer vision, an image captured by an industrial camera comprises multiple neatly arranged pixel points. Take a gray-scale image as an example, an image can be regarded as a 2D matrix, and each set of coordinates corresponds to a gray-scale value between [0, 255]. Considering that the Steger approach is more complicated when calculating the normal direction, therefore, after contemplating the gray-scale image as an array, we consider to introducing the process of data dimensionality reduction approach to calculate the normal directions of the target pixel points.

Principal component analysis (PCA) was proposed by Pearson [15] in 1901, which is a standard approach for data dimensionality reduction. The essence of the approach is to find a suitable coordinate system that reduces the dimensionality of the data under the condition of minimizing data loss. For this purpose, it is necessary to get the coordinate origin、the rotation angle of the new coordinate system, and the coordinates of the data under the new coordinate system. To find the direction of the new coordinate system, the approach's core is to build and solve the covariance matrix. Its mathematical expression is:

$$\mathbf{C}=\begin{bmatrix}\operatorname{cov}(x,x) & \operatorname{cov}(x,y)\\ \operatorname{cov}(x,y) & \operatorname{cov}(y,y)\end{bmatrix}=\begin{bmatrix}\frac{\sum_{i=1}^{n}x_i^2}{n-1} & \frac{\sum_{i=1}^{n}x_iy_i}{n-1}\\ \frac{\sum_{i=1}^{n}x_iy_i}{n-1} & \frac{\sum_{i=1}^{n}y_i^2}{n-1}\end{bmatrix} \tag{2}$$

In Eq. (2), the x_i and y_i are the horizontal and vertical coordinates of the samples within the matrix, respectively. The eigenvector corresponding to the smallest eigenvalue in the covariance matrix is the normal direction of this matrix.

After introducing this idea to extract the center of the light stripe, we can achieve the purpose of calculating the normal direction of the target position. Previously, we [16] used PCA to extract the target stripe center and got a relatively good extraction effect. But PCA needs to calculate the covariance matrix so that there is still room for simplification in terms of computational volume. Singular value decomposition (SVD) is a widely used data dimensionality reduction approach in machine learning. The mathematical expression of SVD is:

$$\mathbf{M}=\mathbf{U}\mathbf{\Sigma}\mathbf{V}^T \tag{3}$$

In Eq. (3), a $m\times n$ matrix $\mathbf{M}$ can be decomposed into $\mathbf{U}$, $\mathbf{\Sigma}$, and $\mathbf{V}$ by SVD, where $\mathbf{U}$ is the eigenvector matrix of $\mathbf{M}\mathbf{M}^T$ with dimension $m\times m$, $\mathbf{V}$ is the eigenvector matrix of $\mathbf{M}^T\mathbf{M}$ with dimension $n\times n$, and $\mathbf{\Sigma}=\begin{bmatrix}\delta_1 & 0 & 0 & \ldots\\ 0 & \delta_2 & 0 & \ldots\\ 0 & 0 & \delta_3 & \ldots\\ \ldots & \ldots & \ldots & \ldots\end{bmatrix}$ is the eigenvalue matrix of $\mathbf{M}\mathbf{M}^T$ or $\mathbf{M}^T\mathbf{M}$ with dimension $m\times n$.

According to the knowledge of data dimensionality reduction, since the matrix $\mathbf{V}$ is equivalent to the covariance matrix of PCA, SVD can also achieve the purpose of calculating the normal direction without calculating the covariance matrix. So it can improve the operational efficiency compared with PCA when we obtain the normal direction of the matrix. Because of the above reasons, we plan to introduce SVD into the extraction process of the center of the line structured light stripe to get the normal direction of the target pixel points, and therefore is the core innovation of this paper. Figure 1 shows the flowchart of the proposed approach, and we will elaborate on the specific derivation process in sections 2.2–2.5.

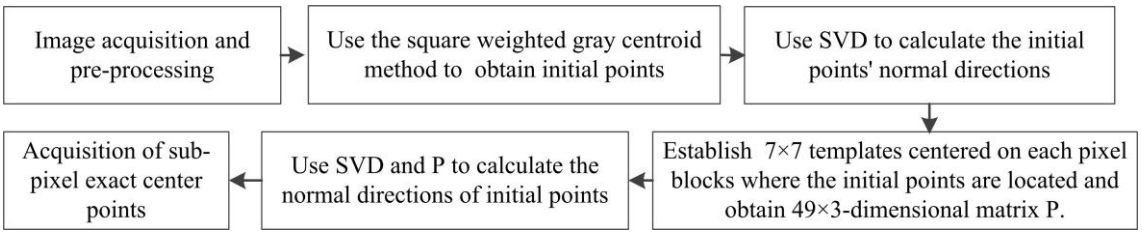

Fig.1 – Flowchart of the approach.

2.2. Image acquisition and pre-processing

Before the extraction of the light stripe center，the acquisition of high-quality images can effectively reduce the complexity of image pre-processing and thus improve the computational speed of the approach. To ensure that we can obtain the high-quality images under actual working conditions, place the industrial

camera mounted with a filter and the line structured light emitter in parallel. Select the relatively weak welding arc spectrum of 610–700 nm as the wavelength, and add a filter to reduce the interference of high-intensity arc light on the line structured light image acquisition. The gray-scale distribution of the image before and after the installation of the filter is shown in Fig. 2. By comparison, the addition of the filter can effectively reduce the influence of the noise generated under the natural light condition on the light stripe.

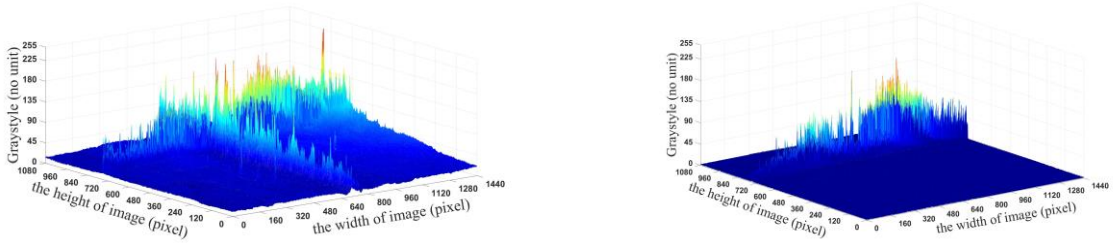

Fig. 2 – Gray-scale distribution before and after adding the filter.

The subsequent work is the pre-processing of the images. As shown in Fig. 2, the line structured light image gets through the filter has removed most of the noise, and the contrast between the light stripe and the background is evident. However, because the surface of the steel plate used for welding is rough, random noise still exists in the region outside the light stripe. Therefore, we use median filter to convolve the image and eliminate the interference of pepper noise. Subsequently, use the adaptive Otsu approach [17] to separate the stripe from the background and obtain the region of interest (ROI). Figure 3 shows the results.

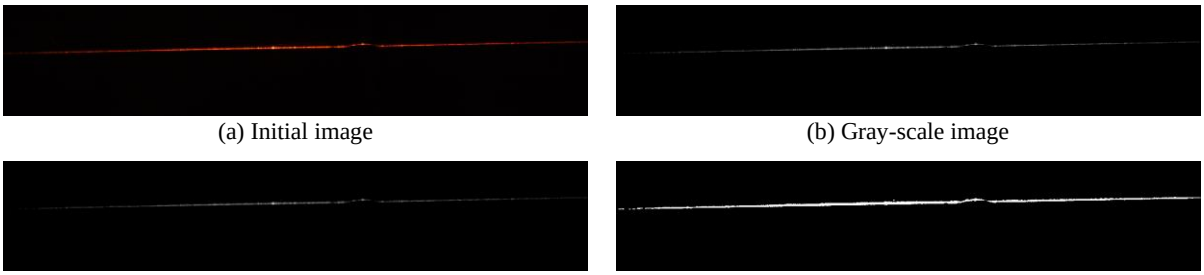

(a) Initial image (b) Gray-scale image

(c) Median filtered image (d) ROI after threshold segmentation

Fig. 3 – Pre-processing results of line structured light stripe image.

2.3. Extraction of initial points

After separating the light stripe from the background to obtain the ROI, most noise within the image has been removed effectively. To provide the reference for the calculation of the normal direction, the next task is the extraction of the initial center point of the light stripe. Because of the Gaussian distribution of stripe light intensity, the pixel points closer to the target center point positions contribute more to finding the center points. Therefore, this paper adopts the square weighted gray centroid approach instead of the traditional gray centroid approach, which makes the obtained initial center points closer to the actual values by increasing the weights of the pixel points more relative to the target center. Its mathematical expression is:

$$Y_c = \frac{\sum_{y=1}^{n} I^2(x,y)y}{\sum_{y=1}^{n} I^2(x,y)} \tag{4}$$

In Eq. (4), Y_c is the longitudinal coordinate of the centroid of the structured light stripe on the cross-section, $I(x,y)$ is the gray value corresponding to the (x,y) coordinate on the image cross-section, and n is the number of pixel points within the cross-section.

2.4. Acquisition of initial points' normal direction

After obtaining the initial points of the structured light stripe, use SVD to calculate the normal directions of the initial points, which is the core innovation of this paper. The width of the light stripes is usually between 3–12 pixels [18]. According to our experiments, the width of the light stripes is mostly 7–8 pixels. Because the light stripe has continuity, considering the surrounding pixels' influence on calculating the points' normal directions, as shown in Fig. 4, establish several 7×7 templates centered on the pixel blocks where the initial points are located. As shown in Fig. 5, use the *x*-axis and *y*-axis coordinates of the pixel blocks within the template and the corresponding gray values to create a 49×3-dimensional matrix $\mathbf{P}$.

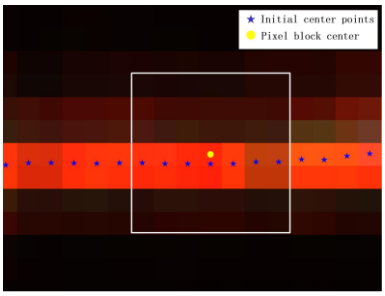

Fig. 4 – Principle of establishing the matrix P required for SVD.

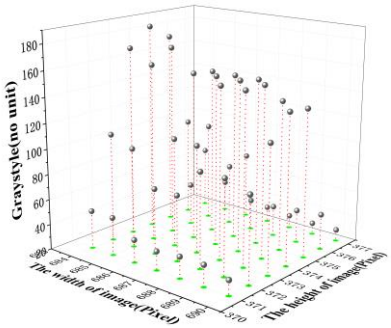

(a) Mapping each gray-scale value to 3D space

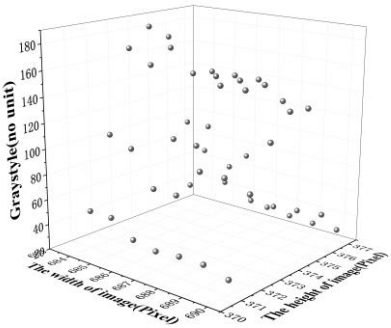

(b) Established 49×3-dimensional matrix $\mathbf{P}$

Fig. 5 – Establishment of matrix $\mathbf{P}$.

Subsequently, after multiplying the respective transpose matrices on both sides simultaneously according to Eq. (4), we can get the equation:

$$\mathbf{P}^T\mathbf{P} = (\mathbf{U\Sigma V}^T)^T\,\mathbf{U\Sigma V}^T = \mathbf{V\Sigma U}^T\mathbf{U\Sigma V}^T \tag{5}$$

Since the matrix $\mathbf{U}$ is orthogonal, the transpose matrix is equal to the inverse matrix can be eliminated, which leads to:

$$\mathbf{P}^T\mathbf{P} = \mathbf{V\Sigma\Sigma V}^T \tag{6}$$

Let $\mathbf{L} = \mathbf{\Sigma\Sigma}$, Eq. (5) can be reduced to:

$$\mathbf{P}^T\mathbf{P} = \mathbf{VLV}^T \tag{7}$$

Since the matrix $\mathbf{V}$ is an orthogonal matrix, the transpose of the $\mathbf{V}$ by multiplying both sides together gives the equation:

$$\mathbf{P}^T\mathbf{PV} = \mathbf{VL} \tag{8}$$

Repeating the above steps, we can obtain the equation below by right multiplying the respective transpose matrix:

$$\mathbf{PP}^T\mathbf{U} = \mathbf{UL} \tag{9}$$

According to the concept of eigenvalues and eigenvectors, $\mathbf{P}^T\mathbf{P}v = \lambda v$, where λ, v are the eigenvalues and eigenvectors of matrix $\mathbf{P}^T\mathbf{P}$, respectively.

The eigenvector sets $\mathbf{V}$ and $\mathbf{U}$ of $\mathbf{P}^T\mathbf{P}$, $\mathbf{P}\mathbf{P}^T$ and the eigenvalue matrix $\mathbf{L}$ are finally obtained by calculation, where $\mathbf{L}=\begin{bmatrix}\delta_1^2 & 0 & 0\\ 0 & \delta_2^2 & 0\\ 0 & 0 & \delta_3^2\\ \cdots & \cdots & \cdots\end{bmatrix}=\begin{bmatrix}\lambda_1 & 0 & 0\\ 0 & \lambda_2 & 0\\ 0 & 0 & \lambda_3\\ \cdots & \cdots & \cdots\end{bmatrix}_{49\times 3}$.

Since $\mathbf{P}$ is a 49×3-dimensional matrix, $\mathbf{P}^T\mathbf{P}$ is a 3×3 matrix, and the eigenvector set $\mathbf{V}$ obtained by solving $\mathbf{P}^T\mathbf{P}$ is also a 3×3 matrix, which contains a new set of orthogonal bases, the directions of the principal components 1, 2, 3 obtained by using the covariance matrix in the PCA approach. The eigenvector corresponding to the minimum eigenvalue is the normal direction of $\mathbf{P}$. As shown in Fig. 6a, the set $i_{\lambda 1}$, $j_{\lambda 2}$ and $k_{\lambda 3}$ is the principal component directions got by the SVD approach, and they are also the directions of the new coordinate system. The principal component $k_{\lambda 3}$ corresponding to the minimum eigenvalue λ_3 is the normal direction of the initial point.

(a) The directions of the new coordinate system (b) Project the normal directions to the x – y plane

Fig. 6 – Acquisition of the initial point normal direction.

As shown in Fig. 6b, let the projected vector onto the x–y plane as the normal direction of the nearest initial point to the pixel block. Set the normal direction $k_{\lambda 3}=(a_1,a_2,a_3)$, then $k'_{\lambda 3}=(a_1,a_2)$ is the projection of $k_{\lambda 3}$ in the x–y plane. Finally, we can obtain the normal direction of the initial point.

Repeat the above work for each initial point until finding the normal directions of all points.

2.5. Acquisition of sub-pixel exact center points

After obtaining the normal directions of the initial center points, set the normal unit vector $\mathbf{n}=\begin{bmatrix}\eta_x & \eta_y\end{bmatrix}^T$. Taking the pixel point with the horizontal coordinate x_c of the image and the vertical coordinate y_c calculated by the weighted gray centroid approach as the coordinate of the initial point, the gray value function is subjected to second-order Taylor expansion along the normal:

$$I(x_c+t\eta_x, y_c+t\eta_y)=I(x_c,y_c)+t\,\mathbf{n}^T\cdot\begin{bmatrix}I_x\\ I_y\end{bmatrix}+\frac{t^2}{2!}\mathbf{n}^T\cdot\begin{pmatrix}I_{xx} & I_{xy}\\ I_{yx} & I_{yy}\end{pmatrix}\cdot\mathbf{n} \tag{10}$$

In Eq. (10), I_x, I_y, I_{xx}, I_{xy}, I_{yx}, I_{yy} are the first and second-order partial derivatives corresponding to the image $I(x,y)$, unlike the Steger method, we use the Sobel operator to calculate the partial derivatives in this paper instead. To ensure that within a pixel, the center of the stripe satisfies the condition that $\left[t\eta_x, t\eta_y\right]\in\left[-\frac{1}{2},\frac{1}{2}\right]\times\left[-\frac{1}{2},\frac{1}{2}\right]$, according to the characteristic that the light stripes satisfy Gaussian distribution, and $\frac{\partial I}{\partial t}=0$, we can obtain:

$$t = -\frac{\eta_x I_x + \eta_y I_y}{\eta_x^2 I_{xx} + 2\eta_x \eta_y I_{xy} + \eta_y^2 I_{yy}} \tag{11}$$

In summary, we use $(x_c + t\eta_x, y_c + t\eta_y)$ to obtain the exact positions of the stripe center.

After obtaining the precise positions of the stripe, in order to make the continuity between the neighboring points, fit the exact center points with cubic spline interpolation. Since the center points at the edge of the image are easily lost during the extraction process, cause distortion of the interpolation curve, and those points do not contain the morphological features of the weld, to eliminate this problem, we decide to reduce the interpolation interval in the process appropriately.

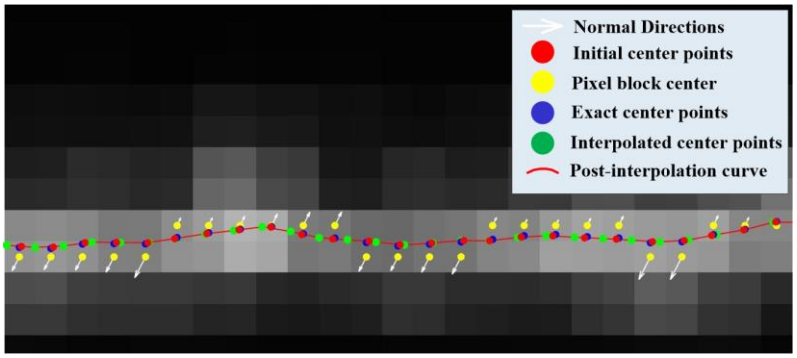

Fig. 7 – Extraction of center points and curve fitting.

Figure 7 shows the extraction of the center after a series of transformations. The yellow, red, blue and green dots in Fig. 7 represent the center of pixel blocks, the initial, exact and interpolated center points respectively, the red curve represents the interpolated centerline, the white arrows represent the normal directions.

3. EXPERIMENTAL RESULTS AND THEIR ANALYSIS

3.1. Light stripe center extraction experiment

The parameters of each equipment of the experimental platform required for image acquisition in this paper are as follows: The wavelength of the line structure light emitter is 650 nm, the industrial camera model is Daheng MER2-160-75GC CMOS industrial camera, the camera lens model is Computar M0814-MP2, and install an AZURE-BP635+-30 nm filter is on the lens, the one-dimensional moving platform with fixed speed movement consists an EG515CA-800 linear guide slide and a D57CME31 servo motor. When the line structured light emitter generates a distorted light stripe on the weld sample, the line structured light images can be captured continuously at a fixed acquisition frame rate by the experimental platform.

Figure 8 shows the results of extracting the centers of several stripes under different positions of the weld sample. It can be seen that the approach in this paper can achieve the extraction of the center under different positions, which meets the expected effect of the experiment.

(a) The structured light without distortions

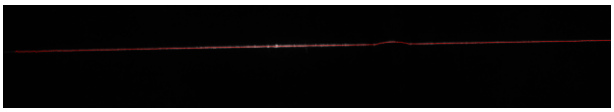

(b) The structured light at the front of the weld

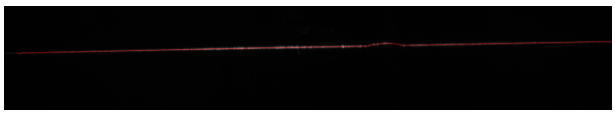

(c) The structured light in the middle of the weld

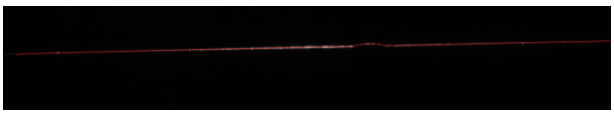

(d) The structured light at the end of the weld

Fig. 8 – Stripe center extraction effect under different positions.

After setting the required variance of the Gaussian convolution kernel for the Hessian matrix to 3 and the gravity threshold for the gray centroid approach and Steger approach to 11, calculate the center using each of the 3 approaches. Figure 9 shows the center extraction results of the stripe in Fig. 8c using the gray centroid approach and the Steger approach, respectively. It can be seen that, because of the influence of noise, the centerline will fluctuate in the local position using the gray centroid approach, which affects the extraction accuracy. In contrast, the extraction effect of the Steger approach with higher accuracy is more stable. The approach in this paper can achieve the same effect of accurate extraction as the Steger approach.

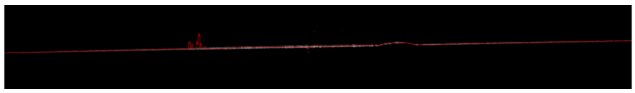

(a) Gray centroid approach

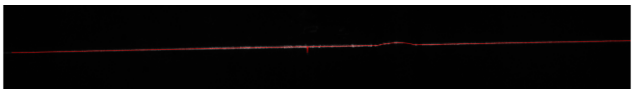

(b) Steger approach

Fig. 9 – Stripe center extraction effect by different approaches.

3.2. Analysis of center extraction accuracy

There is no uniform and clear approach for analyzing the extraction accuracy. Meanwhile, since the true value of the center cannot be measured, the actual error δ is unknown, which leads to the standard error σ of the light stripe center cannot being measured directly [19]. Therefore, in the actual measurement, when the true value is unknown, the residual $v_i = x_i - x$ is commonly used instead of the true difference. The value of σ is obtained using the Bessel formula:

$$\sigma = \sqrt{\frac{\sum_{i=1}^{n} v_i^2}{(n-1)}} \tag{12}$$

According to Eq. (12), Table 1 shows the error values (σ_x, σ_y) of the center coordinate calculated by the Steger approach, the gray centroid approach, and the approach in this paper, respectively.

Table 1

Comparison of light stripe center extraction deviation

The shape of the light stripe	Steger approach	Gray centroid approach	Proposed approach
Fig. 7a	（419.5031，8.8057）	（415.8365，8.6983）	（415.8363，8.7775）
Fig. 7b	（377.3527，7.0634）	（411.5613，7.8676）	（406.0891，7.7081）
Fig. 7c	（391.7558，7.4794）	（414.9933，8.0887）	（406.0931，7.7821）
Fig. 7d	（378.2376，8.0841）	（415.2557，8.9220）	（401.8171，8.5814）

From Table 1, we can conclude that when performing the center extraction for the linear stripe without distortions, the standard error of this approach has little difference with the gray centroid approach. While performing the center extraction for the stripes with distortion, the extraction deviation is reduced to a certain extent compared with that of the gray centroid approach, and it approaches the Steger approach. In general, the approach of this paper can effectively improve the extraction accuracy of the gray centroid approach.

3.3. Program runtime analysis

The computer used for image processing is a DELL Precision T5820 tower graphics workstation with Intel Xeon W-2245 CPU, 3.90GHz, 64G RAM, NVIDIA GeForce RTX 3090 graphics card, and the image processing software is Matlab 2017a. Table 2 shows the comparison results of the running time using the Steger approach、the gray centroid approach, the PCA approach, and the approach in this paper. From Table 2, we can conclude that the approach in this paper can significantly improve the overall computing speed compared with other approaches. The processing time of one image can reduce to about 400ms, so it can better meet the requirement of extracting the center of the stripe in real-time.

Table 2

The proceeding time of each approach

The shape of the light stripe	Steger approach	Gray centroid approach	PCA approach	Proposed approach
Fig. 7a	1.8353 s	0.0398 s	0.4620 s	0.2816 s
Fig. 7b	1.8831 s	0.0355 s	0.5740 s	0.4116 s
Fig. 7c	1.8999 s	0.0470 s	0.5380 s	0.4208 s
Fig. 7d	1.9124 s	0.0417 s	0.5688 s	0.4289 s

3.4. 3D point cloud extraction accuracy analysis

Using the calibrated experimental platform, adjust the industrial camera at a frame rate of 20 FPS, exposure time of 5000 us, and use the 1D moving platform at a speed of 5 mm/s to scan 3 straight weld samples of approximately 50 mm, respectively. After the sub-pixel accuracy center extraction using the approach in this paper, combined with the line-surface model and the laser triangulation approach, finally we can get the 3D point cloud data of the weld surface shown in Fig. 10. In the observation of the recovered 3D point cloud data by using Cloud Compare, it can be seen that the 3D point cloud got by the approach in this paper has good robustness and keeps the local features of the weld sample while minimizing the impact of noisy point clouds on the post-processing.

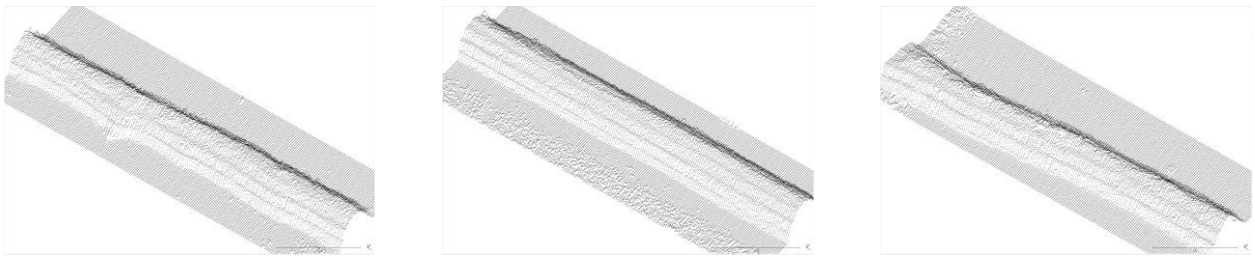

Fig. 10 – Acquired weld point cloud data.

To verify the accuracy of the weld point cloud, first, we measure the width and height of the weld by using the HJC40 weld inspection tape. Then, compare the data with the got point cloud data. Figure 11 shows the measurement results, where the horizontal coordinates represent the image markers, and the vertical coordinates represent the measured width or height values in mm.

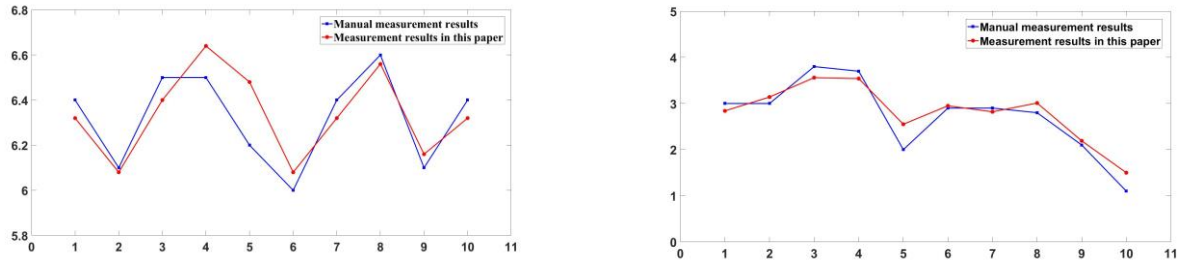

(a) Comparison width dimensions (b) Comparison height dimensions

Fig. 11 – Comparison of weld sample size measurement.

The comparison shows that the manual measurement of the weld sample is prone to measurement errors and has low accuracy. We estimate that the measurement time for a particular weld location during manual measurement is about 20 s. It can't achieve accurate and fast measurement of the sample. The visual measurement of 3D point cloud data got using the center extraction approach proposed in this paper has been substantially improved in terms of both detection accuracy and speed. The measurement time for a specific location has been shortened to about 400 ms, meeting the demand for accurate and fast measurement of weld samples.

4. CONCLUSION

To address the problem that accuracy and speed cannot be reconciled during the line structured light center extraction process, in this paper, the center extraction approach of line structured light stripe is our main research. After analyzing two crucial data dimensionality reduction approaches of PCA and SVD, we proposed an improved extraction approach. Experiments show that this approach can improve the extraction speed and consider the extraction accuracy. It has been proved that this approach can better meet the requirements of industrial real-time detection and provide help for point cloud processing and surface reconstruction in the future. In the future, based on the research in this paper, we can use the collected weld point cloud data to build a dataset and use deep learning networks such as Pointnet++, etc. to classify the weld type and segment the weld from the base material.

ACKNOWLEDGMENTS

This work is supported by the National Natural Science Foundation of China (Grant No. 62073239).

REFERENCES

1. P. DEVENDRAN, S. PRASATH, S. MOHANAN, G. PRAVEEN, *Articulated robotic system-wireless, manual and shadow mode*, Materials Today: Proceedings, **37**, pp. 3194–3198, 2021.
2. C. FANG, M.B. GORDON, S. MUMIN, *Overview of 3-D shape measurement using optical methods*, Optical Engineering, **39**, *1*, pp. 10–22, 2000.
3. S. SON, H. PARK, K.H. LEE, *Automated laser scanning system for reverse engineering and inspection*, International Journal of Machine Tools and Manufacture, **42**, *8*, pp. 889–897, 2002.
4. H. YU, Y. HUANG, D. ZHENG, L. BAI, J. HAN, *Three-dimensional shape measurement technique for large-scale objects based on line structured light combined with industrial robot*, Optik, **202**, art. 163656, 2020.
5. X. XU, Z. FEI, J. YANG, Z. TAN, M. LUO, *Line structured light calibration method and centerline extraction: A review*, Results in Physics, **19**, art. 103637, 2020.
6. P. PERONA, J. MALIK, *Scale-space and edge detection using anisotropic diffusion*, IEEE Transactions on Pattern Analysis and Machine Intelligence, **12**, *7*, pp. 629–639, 1990.
7. B. HU, D. LI, G. JIN, H. HU, *New method for obtaining the center of structured light stripe by direction template*, Computer Engineering and Applications, **11**, pp. 59–60, 2002.
8. P. FASOGBON, L. DUVIEUBOURG, L. MACAIRE, *Fast laser stripe extraction for 3D metallic object measurement*, IECON 2016 – 42nd Annual Conference of the IEEE Industrial Electronics Society, 2016, pp. 923–927.
9. H.F. WANG, Y.F. WANG, J.J. ZHANG, J. CAO, *Laser stripe center detection under the condition of uneven scattering metal surface for geometric measurement*, IEEE Transactions on Instrumentation and Measurement, **69**, *5*, pp. 2182–2192, 2020.
10. H. GAO, G. XU, *Robust analysis and laser stripe center extraction for rail images*, Applied Sciences, **11**, *5*, art. 2038, 2021.
11. C. STEGER, *An unbiased detector of curvilinear structures*, IEEE Transactions on Pattern Analysis and Machine Intelligence, **20**, *2*, pp. 113–125, 1998.
12. K.T. DIEDRICH, J.A. ROBERTS, R.H. SCHMIDT, D.L. PARKER, *Comparing performance of centerline algorithms for quantitative assessment of brain vascular anatomy*, Anatomical Record, **295**, *12*, 2179–2190, 2012.
13. Z.X. HU, H.T. ZHU, M. HU, Y. MA, *Adaptive centre extraction method for structured light stripes*, Ukrainian Journal of Physical Optic, **18**, *1*, pp. 9–19, 2017.
14. J. LIU, L. LIU, *Laser stripe center extraction based on hessian matrix and regional growth*, Laser & Optoelectronics Progress, **56**, *02*, pp. 113–118, 2019.
15. K. PEARSON, *LIII. On lines and planes of closest fit to systems of points in space*, Philosophical Magazine, **2**, *11*, pp. 559–572, 1901.
16. Q. ZHENG, Q. LIU, P. ZHU, W. MA, J. LIU, X. LI, *Study on the centerline extraction method on weld image line structured light stripe*, UPB Scientific Bulletin, Series C: Electrical Engineering and Computer Science, **84**, *1*, pp. 21–32, 2022.
17. N. OTSU, *A threshold selection method from gray-level histograms*, IEEE Transactions on Systems, Man, and Cybernetics, **9**, *1*, pp. 62–66, 1979.
18. J. YANG, X. YANG, S. CHENG, Z. LEI, S. LUO, X. ZHANG, *Review of extracting the centers of linear structured light stripes for 3D visual measurements*, Journal of Guangdong University of Technology, **31**, *01*, pp. 74–78, 2014.
19. W. LI, G. PENG, X. GAO, C. DING, *Fast extraction algorithm for line laser strip centers*, Chinese Journal of Lasers, **47**, *03*, pp. 192–199, 2020.

Received September 22, 2022